

# Facile construction of ZnNi<sub>2</sub>O<sub>4</sub> materials as high-performance anode for lithium-ion capacitors<sup>#</sup>

Xinrong Lv<sup>1,2</sup>, Junsheng Zheng<sup>1,2\*</sup>

1 Clean Energy Automotive Engineering Center, Tongji University, Jiading District, Shanghai 201804, China

2 College of Automotive Studies, Tongji University, Jiading District, Shanghai 201804, China

(Corresponding Author: [jszheng@tongji.edu.cn](mailto:jszheng@tongji.edu.cn))

## ABSTRACT

In this paper, a ZnNi<sub>2</sub>O<sub>4</sub> anode material is prepared by a simple hydrothermal reaction process for lithium-ion capacitors. Bimetallic oxides exhibit excellent specific capacity and cycle stability based on redox reactions of different metals. The morphology, composition and structure of ZnNi<sub>2</sub>O<sub>4</sub> are characterized by X-ray diffraction, transmission electron microscope and X-ray photoelectron spectroscopy. At a current density of 0.1 A g<sup>-1</sup>, the ZnNi<sub>2</sub>O<sub>4</sub> has a high initial specific capacity of 1244.73 mAh g<sup>-1</sup>. Even when the current density is 1 A g<sup>-1</sup>, the specific capacity of ZnNi<sub>2</sub>O<sub>4</sub> is still as high as 342.41 mAh g<sup>-1</sup>. It is worth noting that the excellent electrochemical results indicate that ZnNi<sub>2</sub>O<sub>4</sub> is a promising anode candidate for lithium-ion capacitors.

**Keywords:** ZnNi<sub>2</sub>O<sub>4</sub>, bimetallic oxides, lithium-ion capacitor, anode material

## NONMENCLATURE

### Abbreviations

Li	Lithium
AC	Activated carbon
Zn	Zinc
Ni	Nickel
Ga	Gallium
Cu	Cuprum
Ti	Titanium
Fe	Ferrum
Mn	Manganese
EC	Ethylene carbonate
DMC	Dimethyl carbonate
Ar	Argon
Sat.	Satellites

### Symbols

h	Hour
ppm	Parts per million

mg	Milligram
M	Mole
mL	Milliliters
mm	Millimeter
V	Volt

## 1. INTRODUCTION

With the intensification of environmental problems and the increasing demand for energy, it is urgent to develop and research sustainable energy [1]. Lithium-ion capacitors have attracted much attention because they combine the high power density of supercapacitors with the high energy density of lithium-ion batteries [2]. Electrode materials are one of the key components of Lithium-ion capacitors, so it is important to develop anode materials with high specific capacitance and high performance of Lithium-ion capacitors.

Transition metal oxides are used as anodes for Lithium-ion capacitors because of their high specific capacitance, ecological friendliness, low cost, simple preparation, high safety and excellent performance. Common bimetallic oxides include MnCo<sub>2</sub>O<sub>4</sub>, NiGa<sub>2</sub>O<sub>4</sub>, NiCo<sub>2</sub>O<sub>4</sub> [3] and NiFe<sub>2</sub>O<sub>4</sub> [4]. Fan et al. synthesized TiO<sub>2</sub>/MnCo<sub>2</sub>O<sub>4</sub> by solvothermal method. The addition of tubular TiO<sub>2</sub> alleviates the agglomeration phenomenon of MnCo<sub>2</sub>O<sub>4</sub>, thus shortening the diffusion path of lithium ions. The TiO<sub>2</sub>/MnCo<sub>2</sub>O<sub>4</sub> composite showed excellent capacitance of 743 mAh g<sup>-1</sup> and excellent rate performance as an anode. It is further assembled with activated carbon electrode as cathode to form Lithium-ion capacitor. Lithium-ion capacitor provides high energy densities of 89.8 and 44.1 Wh kg<sup>-1</sup> at power densities of 0.25 and 3.41 kW kg<sup>-1</sup>, respectively [5]. He et al. synthesized a nano-flower-shaped NiGa<sub>2</sub>O<sub>4</sub> through hydrothermal reaction and calcination process. NiGa<sub>2</sub>O<sub>4</sub> not only has alloy reaction to produce Ga, but also has a

<sup>#</sup> This is a paper for the 16th International Conference on Applied Energy (ICAE2024), Sep. 1-5, 2024, Niigata, Japan.

hybrid energy storage mechanism including conversion reaction to produce Ni. These two energy storage mechanisms make NiGa<sub>2</sub>O<sub>4</sub> show excellent performance. NiGa<sub>2</sub>O<sub>4</sub>//AC lithium-ion capacitor device is composed of NiGa<sub>2</sub>O<sub>4</sub>//AC as anode and activated carbon as cathode. The device exhibits excellent energy density and power density performance, with a high energy density of 104.89 Wh kg<sup>-1</sup> (200 W kg<sup>-1</sup>) and a high power density of 3999 W kg<sup>-1</sup> (25.44 Wh kg<sup>-1</sup>) [6]. Bimetallic oxides, especially ZnNi<sub>2</sub>O<sub>4</sub>, have excellent specific capacitance and electrochemical properties due to various redox states and different redox reactions.

In this paper, we propose a bimetallic oxide ZnNi<sub>2</sub>O<sub>4</sub> as anode material for Li-ion capacitors. The material was synthesized by simple control of the molar ratio of Zn and Ni precursors and hydrothermal reaction. The bimetallic oxide ZnNi<sub>2</sub>O<sub>4</sub> alleviates the volume expansion and contraction of lithium-ion capacitors in the process of charge and discharge by using the complementary and synergistic interaction between different metals. Bimetallic oxide ZnNi<sub>2</sub>O<sub>4</sub> shows excellent capacitance and electrochemical properties and is an excellent anode material for lithium ion capacitors.

## 2. EXPERIMENTAL

### 2.1 Chemicals

NiSO<sub>4</sub>·6H<sub>2</sub>O, ZnSO<sub>4</sub>·7H<sub>2</sub>O, urea were obtained from Macklin Co., Ltd. (ShangHai, China) without further purification.

### 2.2 Preparation of ZnNi<sub>2</sub>O<sub>4</sub>

Preparation of ZnNi<sub>2</sub>O<sub>4</sub>: 0.1 mol NiSO<sub>4</sub>·6H<sub>2</sub>O and 0.05 mol ZnSO<sub>4</sub>·7H<sub>2</sub>O were added into 75 mL ultra-pure water for 6 h. Then 0.2 mol of urea was added and stirred continuously for 7 h. The prepared solution was added to 150 mL teflon-lined autoclave and reacted at 120°C for 36 h. After cooling, the prepared powder sample is taken out and cleaned several times with ultra-pure water and ethanol. Finally, the samples were put into a vacuum drying oven and dried at 70°C for 12 h.

### 2.3 Material characterizations

The crystal structures of ZnNi<sub>2</sub>O<sub>4</sub> was characterized by X-ray diffraction at the scanning rate of 10° min<sup>-1</sup> in the range of 10–90° of 2θ with Rigaku-D/Max-2550PC (Japan). The chemical states of the surface elements of ZnNi<sub>2</sub>O<sub>4</sub> was measured by X-ray photoelectron spectroscopy with Thermo Scientific of Escalab 250Xi. The morphology of electrode material ZnNi<sub>2</sub>O<sub>4</sub> was studied by JEM-2100F transmission electron microscope (Japan).

## 2.4 Electrochemical measurement

The ZnNi<sub>2</sub>O<sub>4</sub> anode were prepared by blade coating method. The specific preparation process of ZnNi<sub>2</sub>O<sub>4</sub> is as follows: the ZnNi<sub>2</sub>O<sub>4</sub>, Super P and Polyvinylidene fluoride are mixed at a ratio of 80:10:10. Then a certain amount of N-methyl pyrrolidone solvent is added to mix it to form a uniform slurry. The prepared uniform slurry is further coated on the Cu foil. Finally, the slurry was vacuum-dried at 80 °C for 12 h and drilled into a disc with a diameter of 12 mm. The surface loads of ZnNi<sub>2</sub>O<sub>4</sub> electrodes prepared by this method are about 2 mg cm<sup>-2</sup>. ZnNi<sub>2</sub>O<sub>4</sub>/Li half cells (standard CR2032) are prepared in an Ar glove box with oxygen and water content of less than 1.0 ppm. In the process of preparing the half cell, separators use the microporous glass microfiber filter (Whatman GF/C), and the electrolyte consists of 1 M LiPF<sub>6</sub> in the EC and DMC, with a volume ratio of 1:1. It is worth noting that the preparation process of all cells is standardized by adding 100 μL electrolyte.

## 3. RESULTS AND DISCUSSION

### 3.1 Characterization of ZnNi<sub>2</sub>O<sub>4</sub>

In order to understand the crystal structure of ZnNi<sub>2</sub>O<sub>4</sub>, it was characterized by X-ray diffraction in the range of 10-90°. By analyzing the X-ray diffraction pattern of ZnNi<sub>2</sub>O<sub>4</sub>, it can be seen from Fig. 1 that the characteristic peaks are located at 31.7°, 34.5° and 47.4° corresponding to the (100), (002) and (102) crystal plane of ZnO, respectively (marked in blue) according to JCPDS card number of 79–0208. The characteristic peak at 62.8° corresponds to the (220) crystal plane of NiO (marked in green) according to JCPDS card number of 78–0423. The characteristic peaks at 36.9 and 42.8 correspond to the (110) and (200) crystal plane of ZnNi<sub>2</sub>O<sub>4</sub> with d-spacing of 2.4 Å and 2.08 Å, respectively (mark in black) [7].

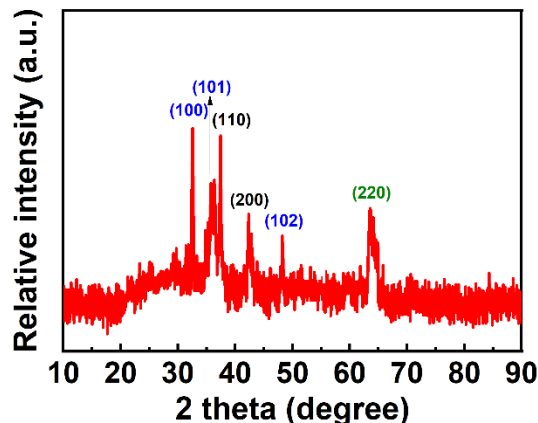


Fig. 1. The X-ray diffraction image of ZnNi<sub>2</sub>O<sub>4</sub>

The specific surface area and pore size distribution of  $\text{ZnNi}_2\text{O}_4$  were further determined and analyzed. The specific surface area of  $\text{ZnNi}_2\text{O}_4$  was determined by Bruauer-Emmet-Teller (BET) method and the pore size distribution of  $\text{ZnNi}_2\text{O}_4$  was determined by Barrett-Joyner-Halenda (BJH) method. Fig. 2A shows the  $\text{N}_2$  adsorption-desorption isotherm of  $\text{ZnNi}_2\text{O}_4$ . It can be seen from the figure that  $\text{ZnNi}_2\text{O}_4$  is a H3-type hysteresis loop, indicating that it is a type IV adsorption and desorption isotherm. The specific surface area of  $\text{ZnNi}_2\text{O}_4$  is  $10.47 \text{ m}^2 \text{ g}^{-1}$ . The pore size distribution of  $\text{ZnNi}_2\text{O}_4$  is shown in Fig. 2B. It can be seen from the pore size distribution that the pore size of  $\text{ZnNi}_2\text{O}_4$  is about 17.32 nm. In conclusion,  $\text{ZnNi}_2\text{O}_4$  has a large specific surface area and its pore size is conducive to increasing the contact between electrolyte and electrode interface, providing more active sites for the storage of lithium ions, thus improving the capacitance and electrochemical performance of  $\text{ZnNi}_2\text{O}_4$ .

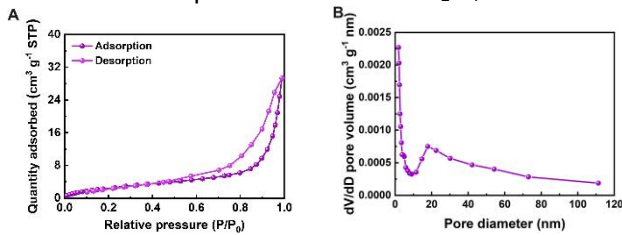


Fig. 2. (A) The  $\text{N}_2$  adsorption-desorption isotherms of  $\text{ZnNi}_2\text{O}_4$ ; (B) pore size distributions of  $\text{ZnNi}_2\text{O}_4$

The elemental and valence states of  $\text{ZnNi}_2\text{O}_4$  were characterized by X-ray photoelectron spectroscopy, and the results are shown in Fig. 3. According to the results of Fig. 3A, it can be seen that electrode material  $\text{ZnNi}_2\text{O}_4$  contains elements Ni, Co, and O. The high-resolution X-ray photoelectron spectroscopy spectrum of O 1s is shown in Fig. 3B, with two peaks at around 530.8 eV and 533.1 eV attributed to metal-oxygen bonds (Zn/Ni-O) and other oxygen types, including  $\text{H}_2\text{O}$  in adsorbed air. In the high-resolution X-ray photoelectron spectroscopy spectra of Zn 2p (Fig. 3C), two characteristic peaks of spin orbits were observed at 1021.5 eV and 1044.8 eV, corresponding to Zn  $2p_{3/2}$  and Zn  $2p_{1/2}$ , respectively, demonstrating the presence of  $\text{Zn}^{2+}$  [7]. The high-resolution X-ray photoelectron spectroscopy spectrum of Ni 2p is shown in Fig. 3D. There are obvious peaks at 855.5 eV and 873.8 eV, corresponding to Ni  $2p_{3/2}$  and Ni  $2p_{1/2}$  respectively, indicating the presence of  $\text{Ni}^{2+}$  and  $\text{Ni}^{3+}$ . It is worth noting that there are clear peaks at 861.9 eV and 879.8 eV for the two shake-up satellites [8].

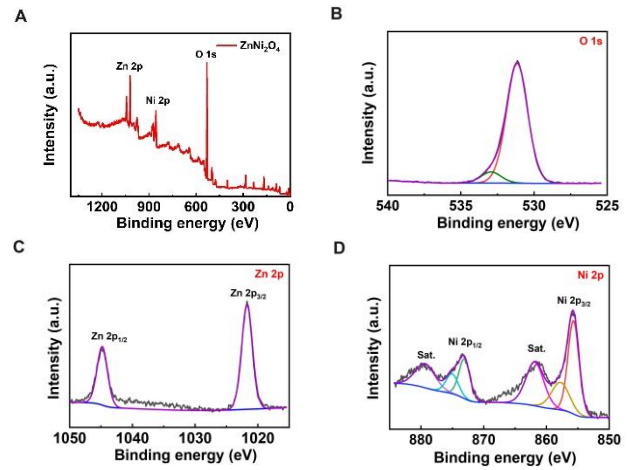


Fig. 3. (A) X-ray photoelectron spectroscopy full spectrum of  $\text{ZnNi}_2\text{O}_4$ ; High-resolution XPS spectrum of (B) O 1s; (C) Zn 2p and (D) Ni 2p for  $\text{ZnNi}_2\text{O}_4$ .

The morphology of electrode material  $\text{ZnNi}_2\text{O}_4$  was studied by transmission electron microscope test. As can be seen from Fig. 4,  $\text{ZnNi}_2\text{O}_4$  presents a nanorod-like structure. The rod-like structure of  $\text{ZnNi}_2\text{O}_4$  is about 450 nm in length and 125 nm in width. The nanorod structure of  $\text{ZnNi}_2\text{O}_4$  can shorten the migration path of lithium ions and alleviate the volume expansion effect of electrode materials during the charge and discharge process, thus promoting the rate performance and cycle stability of lithium ion capacitors.

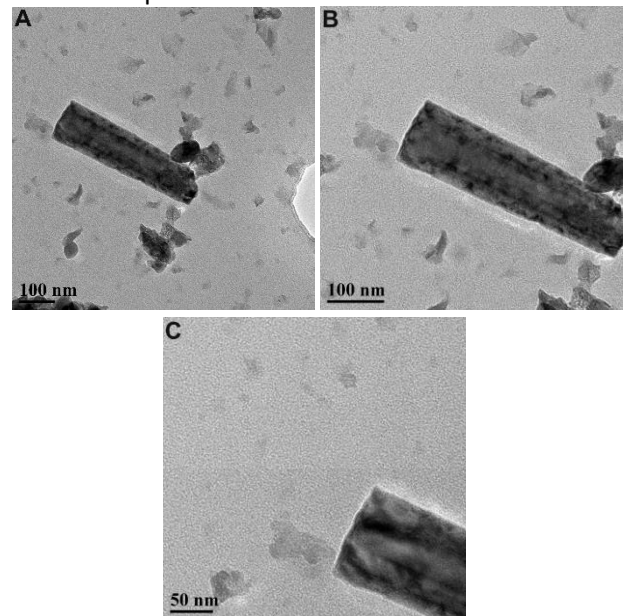
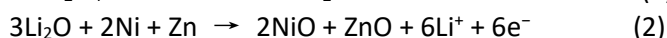
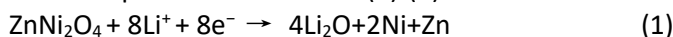


Fig. 4. The transmission electron microscope image of  $\text{ZnNi}_2\text{O}_4$

### 3.2 Electrochemical properties of $\text{ZnNi}_2\text{O}_4$

The electrochemical properties of  $\text{ZnNi}_2\text{O}_4$  were tested in a standard half cell. The lithium storage performance of electrode material  $\text{ZnNi}_2\text{O}_4$  as anode of lithium-ion capacitors was studied. Cyclic voltammetry

test was performed on  $\text{ZnNi}_2\text{O}_4$  at a scanning rate of  $0.2 \text{ mV s}^{-1}$  in the voltage range of 0.01-3 V. As shown in Fig. 5A, there is a wide cathodic peak at 0.43 V, which may be attributed to the reduction of  $\text{ZnNi}_2\text{O}_4$  to metals Zn and Ni, the specific reduction process is shown in the formula (1). During the subsequent sweeping process, the cathodic peak moved to a lower potential and increased in intensity, which may be related to the incomplete infiltration of the electrode and the formation of the solid electrolyte interface. The anodic peak at 1.25 V is associated with the oxidation of metals Zn and Ni to  $\text{Zn}^{2+}$  and  $\text{Ni}^{3+}$ . The entire electrochemical process of  $\text{ZnNi}_2\text{O}_4$  can be expressed as formulas (1)-(2).



The first five times of constant current charge and discharge of  $\text{ZnNi}_2\text{O}_4$  were tested under the current density of  $0.1 \text{ A g}^{-1}$  and voltage range of 0.01-3 V. As can be seen from Fig. 5B, the initial charging capacity of  $\text{ZnNi}_2\text{O}_4$  is  $1728.0 \text{ mAh g}^{-1}$  and the coulomb efficiency is 76.6%. The low initial coulomb efficiency of  $\text{ZnNi}_2\text{O}_4$  may be caused by the formation of solid electrolyte interface film [9]. Fig. 5C shows the charge and discharge curves of the electrode material  $\text{ZnNi}_2\text{O}_4$  at different current densities. As can be seen from Fig. 5C, the charge and discharge curves of the electrode material  $\text{ZnNi}_2\text{O}_4$  at different current densities all show similar shapes, indicating that the electrode material  $\text{ZnNi}_2\text{O}_4$  has good electrochemical reversibility. Fig. 5D shows the rate performance of  $\text{ZnNi}_2\text{O}_4$ . As can be seen from Fig. 5D, when the current density is 0.1, 0.2, 0.3, 0.4, 0.5, 0.6, 0.7, 0.8, 0.9 and  $1.0 \text{ A g}^{-1}$ , the capacitance value of  $\text{ZnNi}_2\text{O}_4$  is 1244.73, 684.37, 543.56, 476.79, 437.63, 409.96, 389.01, 371.7, 356.93 and  $342.4 \text{ mAh g}^{-1}$ , respectively.

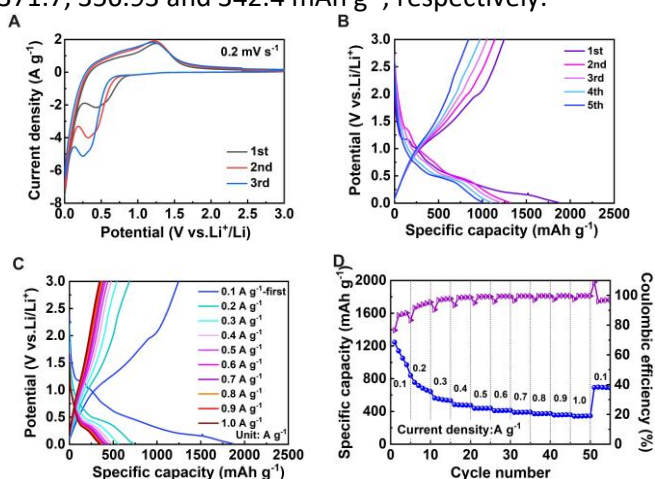


Fig. 5. (A) The CV curves of  $\text{ZnNi}_2\text{O}_4$  at a scan rate of  $0.2 \text{ mV s}^{-1}$ , (B) Charge/discharge curves of  $\text{ZnNi}_2\text{O}_4$  at a current density of  $0.1 \text{ A g}^{-1}$ . (C) Charge/discharge curves

of  $\text{ZnNi}_2\text{O}_4$  at the different current density. (D) Rate performances from  $0.1$  to  $1 \text{ A g}^{-1}$  of  $\text{ZnNi}_2\text{O}_4$ .

#### 4. CONCLUSIONS

In summary, the advantages of bimetallic oxides as anodes for lithium-ion capacitors include high capacity and a variety of redox states. A rod-like electrode material  $\text{ZnNi}_2\text{O}_4$  was synthesized by a simple hydrothermal reaction. Through a series of tests,  $\text{ZnNi}_2\text{O}_4$  shows excellent electrochemical properties, including high charge-discharge capacity and good rate performance. At a current density of  $0.1 \text{ A g}^{-1}$ ,  $\text{ZnNi}_2\text{O}_4$  has a high initial specific capacity of  $1244.73 \text{ mAh g}^{-1}$ . The excellent performance of electrode material  $\text{ZnNi}_2\text{O}_4$  makes it a promising anode for lithium-ion capacitors.

#### ACKNOWLEDGEMENT

The work was sponsored by the financial support from the National Natural Science Foundation of China (52307249), National Science Foundation of Shanghai Province (23ZR1465900), Fundamental Research Funds for the Central Universities at Tongji University (PA2022000668, 22120220426), International Exchange Program for Graduate Students, Tongji University.

#### REFERENCE

- [1] Zhu CY, Mao JJ, Zhao JY, Xu Y, Li G, Li JD, Cheng F. Interface engineering to construct heterostructured  $\text{SnS}_2/\text{Sb}_2\text{S}_3$  on rGO through a targeted-complexation deposition strategy for high-performance lithium-ion capacitors. *Chem Eng J* 2024;493:152702.
- [2] Xu XY, Zhang J, Zhang ZH, Lu GD, Cao W, Wang N, Xia YM, Feng QL, Qiao SL. All-covalent organic framework nanofilms assembled lithium-ion capacitor to solve the imbalanced charge storage kinetics. *Nano-Micro Lett* 2024;16:116.
- [3] Lovett AJ, Daramalla V, Sayed FN, Nayak D, de h-Ora M, Grey CP, Dutton SE, MacManus-Driscoll JL. Low temperature epitaxial  $\text{LiMn}_2\text{O}_4$  cathodes enabled by  $\text{NiCo}_2\text{O}_4$  current collector for high-performance microbatteries. *ACS Energy Lett* 2023;8:3437-3442.
- [4] Du WQ, Zheng YQ, Liu XY, Cheng J, Zeb A, Lin XM, Luo YF, Reddy RCK. Oxygen-enriched vacancy spinel  $\text{MFe}_2\text{O}_4/\text{carbon}$  ( $\text{M} = \text{Ni}, \text{Mn}, \text{Co}$ ) derived from metal-organic frameworks toward boosting lithium storage. *Chem Eng J* 2023;451:138626.
- [5] Fan LQ, Huang JL, Wang YL, Geng CL, Sun SJ, Huang YF, Lin JM, Wu JH.  $\text{TiO}_2$  nanotubes supported ultrafine  $\text{MnCo}_2\text{O}_4$  nanoparticles as a superior-performance anode for lithium-ion capacitors. *Int J Hydrogen Energy* 2021;46:35330-35341.



- [6] He ZH, Gao JF, Kong LB. NiGa<sub>2</sub>O<sub>4</sub> Nanosheets in a microflower architecture as anode materials for li-ion capacitors. *ACS Appl Nano Mater* 2020;2:6238.
- [7] Koudahi MF, Naji L. Hydrothermal synthesis of nickel foam-supported spinel ZnNi<sub>2</sub>O<sub>4</sub> nanostructure as electrode materials for supercapacitors. *Electrochim Acta* 2022;434:141314.
- [8] Zhao J, Zhou CL, Li YJ, Cheng K, Zhu K, Ye K, Yan J, Cao DX, Xie Y, Wang GL. Nickel cobalt oxide nanowires-modified hollow carbon tubular bundles for high-performance sodium-ion hybrid capacitors. *Int J Energ Res* 2020;44: 3883-3892.
- [9] Sahoo G, Senthamaraikannan TG, Jeong HS, Bandyopadhyay P, Lim DH, Nayak SK, Jeong SM. An effective lithium incorporation strategy to boost the charge-storage capacity of bimetallic metal-organic frameworks with theoretical insights and solid-state lithium-ion capacitors. *J Mater Chem A* 2024.